# Effect of Amphiphilic Additives on Nucleation of Hexahydro-1,3,5- trinitro-1,3,5-triazine

**ARTICLE** *in* CRYSTAL GROWTH & DESIGN · NOVEMBER 2013

Impact Factor: 4.89 · DOI: 10.1021/cg4006423



**4 AUTHORS**, INCLUDING:

Jun-Woo Kim
CJ CheilJeDang Bio
**18** PUBLICATIONS **169** CITATIONS

SEE PROFILE

CRYSTAL GROWTH & DESIGN

Article

pubs.acs.org/crystal

# Effect of Amphiphilic Additives on Nucleation of Hexahydro-1,3,5-trinitro-1,3,5-triazine

Jun-Woo Kim, Ji-Hwan Park, Hong-Min Shim, and Kee-Kahb Koo*

Department of Chemical and Biomolecular Engineering, Sogang University, Seoul 121-742, Korea

**ABSTRACT:** Amphiphilic compounds such as oleylamine, oleyl alcohol, and *N*-dodecyl-2-pyrrolidone (NDP) were found to clearly promote the nucleation of hexahydro-1,3,5-trinitro-1,3,5-triazine (RDX) from acetone. A statistical approach of induction time distribution of RDX showed that the nucleation rate increases significantly with addition of a small amount of amphiphilic additives, and experimental data were found to be well-represented by a compressed exponential model with an average induction time of a nonhomogeneous Poisson process. Molecular simulation also supported the fact that the molecular aggregates of RDX are easily covered by those additives, and thus interfacial energy seems to be reduced by the additives embedded onto the crystal surface.

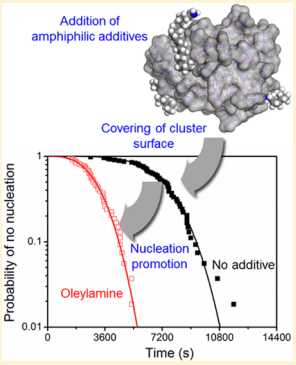


## INTRODUCTION

Nucleation is an essential step in the control of crystal size, size distribution, and polymorphic composition in crystallization processes.[1] Nucleation agents have a strong influence on the nucleation kinetics by adsorbing onto the surface of growing clusters and/or changing the physicochemical nature of the solution, such as solubility and viscosity. When the nucleation agent molecules are adsorbed onto the cluster, the interfacial energy of the growing cluster sometimes decreases (nucleation promotion) or the structural organization of the cluster into an ordered crystal lattice is hindered (nucleation retardation or inhibition).[2−7]

Sangwal reported a semiempirical model for interpreting the effect of additives on nucleation kinetics in cooling crystallization.[2−4] Assuming that the nucleation agent has an influence on both the kinetics and the thermodynamic parameters of the nucleation rate, he attempted to deduce the effect of a nucleation agent on the nucleation rate by induction time measurements in the experiments on cooling crystallization. However, his model does not provide direct information on the physicochemical interaction between the additives and clusters.

Anwar et al. proposed a molecular simulation technique based on the Lennard−Jones system, which consists of simple solute, solvent, and additive spheres, to explain the effect of additives on nucleation.[5] They reported that a solute-philic monomer penetrates into the emerging cluster and retards the nucleation.[6] This would also be the theoretical basis of nucleation retardation or inhibition by solute-philic polymeric additives. Let us imagine that a solute molecule is easily adsorbed onto any part of a polymer molecule bearing many functional groups, which have strong interactions (e.g., hydrogen bonding) with solute molecules along the backbone of the chain. Thus, the penetration of polymer molecules into the growing cluster disrupts the packing of solute molecules into a crystal lattice. Anwar et al. stated another interesting result that amphiphilic dimers tend to reside at the surface of a cluster and they promote the nucleation by decreasing the crystal/solution interfacial energy.[6] This provides a clue for the general explanation on the promotion of nucleation by additives in solution. However, the design of amphiphilic nucleation promoters for the application in the crystallization processes is still facing difficulties because of lack of experimental evidence.

The crystallization processes for energetic materials with nano/submicrometer-size, including grinding and milling, nozzle-assisted drowning-out, supercritical fluidic crystallization, and spray-assisted evaporation crystallization have been extensively investigated to reduce their sensitivity without loss in performance.[8−18] In those experiments, additives are applied as a morphology modifier, a particle binder, a dispersant, or an agglomeration inhibitor.[15−18]

In particular, Kim et al. investigated the effect of nucleation promotion or retardation on crystal habit in the evaporation crystallization of hexahydro-1,3,5-trinitro-1,3,5-triazine (RDX) from atomized droplets in detail.[18] They showed that nonspherical agglomerated particles are formed when a crystal-containing droplet is merged with other droplets or crystals formed already, and a number of nucleation agents are effectively applied as a habit modifier in the crystallization of submicrometer-sized RDX. For instance, oleylamine was shown to decrease the metastable zone width of RDX in cooling crystallization from acetone with no significant change in the nature of the solution. The molecular structures of RDX and oleylamine are depicted in Figure 1 (panels a and b). It is

**Received:** April 27, 2013
**Revised:** September 6, 2013
**Published:** September 12, 2013

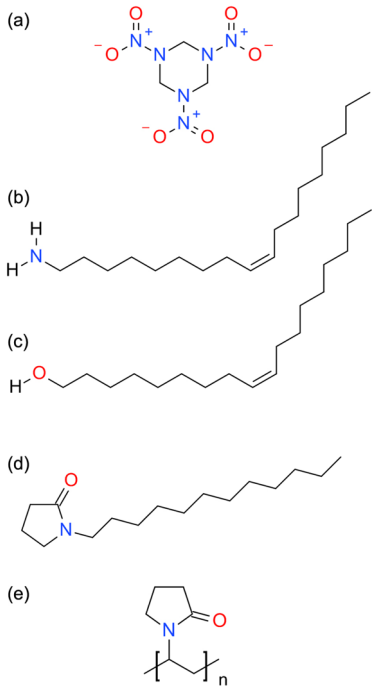


**Figure 1.** Chemical structures of (a) RDX, (b) oleylamine, (c) oleyl alcohol, (d) *N*-dodecyl-2-pyrrolidone (NDP), and (e) polyvinylpyrrolidone (PVP).

expected that oleylamine is an amphiphilic nucleation agent because the functional headgroup of oleylamine may have high affinity with the three nitro groups of RDX molecules by hydrogen bonds, such as H(amine group)−O(RDX) and H(amine group)−N(RDX), whereas the hydrocarbon chain of oleylamine cannot strongly interact with RDX molecules. In the present work, in order to examine quantitatively the effect of an additive on the nucleation rate, the measurements of induction time of RDX nucleation were carried out with addition of oleylamine, oleyl alcohol, and *N*-dodecyl-2-pyrrolidone (NDP). Molecular structures of oleyl alcohol and NDP are also expected as an amphiphilic (Figure 1, panels c and d) like olyelamine.

## EXPERIMENTAL SECTION

**Materials.** RDX (99.9%) was supplied by Hanwha Company (Korea) and was purified before the experiments by the following: (1) Dissolve 50 g of RDX into 1 kg of acetone. (2) Filter the RDX/acetone solution to separate solid impurities. (3) Add 2 kg of water into the solution for the drowning-out of the RDX crystals. (4) Agitate the RDX/acetone/water mixed suspension for 30 min. (5) Filter the suspension and wash RDX with water. (6) Dry more than 2 days.

Acetone (99.5+%), NDP (99%), oleylamine (70%), oleyl alcohol (85%), *n*-butyl alcohol (99.8%), and *n*-butylamine (99.5%) were purchased from Sigma-Aldrich (St. Louis, MO). Polyvinylpyrrolidone (PVP; molecular weight: 40000) was purchased from Tokyo Chemical Industry. The triple-distilled water was produced by a distillation apparatus.

**Measurements of Solubility.** At a fixed temperature, RDX (roughly 0.001 g) was added into acetone (100 g) with or without additives in a jacketed vessel with continuous stirring. This process was repeated until the RDX was not dissolved completely within the time interval of 2 h. The total amount of the solute added was used to estimate solubility. Temperature was controlled by a thermostat bath (Polyscience, model 9712) and the temperature was measured and recorded every 5 s by a data logger (Pico technology, PT-104) equipped with an immersion-type platinum resistance thermometer (Pico technology, SE012, UK; accuracy: ± 0.03 K).

**Measurements of Induction Time.** On the basis of the solubility at 283.15 K, the RDX/acetone solution with a certain supersaturation ratio, *S*, was prepared in a 3 mL vial using an analytical balance (Mettler Toledo, AG204) with an uncertainty of 0.1 mg. At 283.15 K, solubility of RDX in acetone was 5.63 g/100 g acetone and those with oleyl alcohol, NDP and PVP (0.05 wt % on a solute free basis) were 5.61, 5.60, and 5.57 g/100 g acetone, respectively.

Measurements of induction time were carried out without agitation. To repeat the measurements 54 times at each supersaturation, the vial was kept in a water bath at 323.15 K for 2 h for the complete dissolution of RDX and then the vial was quickly immersed into a cold water bath with 283.15 K. Temperatures of the heating and cooling baths were controlled by two thermostat baths. The elapsed time from the moment of vial immersion into a cold bath at 283.15 K to the appearance of the first nucleus detected by a naked eye was recorded as the induction time, and thus size of the crystal detected may be about 1−10 $\mu$m.[19] By an immersion type platinum resistance thermometer with careful sealing after induction time measurements, the temperature of solution in the vial was rechecked and found to be stable with an accuracy of ±0.1 K. In addition, the uniform temperature profiles for the dissolution and the quenching were always kept to reduce the effect of thermal history on nucleation.

**Simulation of Molecular Aggregation Pattern.** To understand the interactions between RDX and additive molecules, the molecular simulation work was made. The COMPASS forcefield was used to model RDX and nucleation agents [oleylamine, oleyl alcohol, NDP, and PVP (repeating unit: 15)]. Each simulation system was set to about 8.3 × 8.3 × 8.3 nm, comprising 150 RDX and 6 nucleation agent molecules. Their initial structures were relaxed by energy minimization, and molecular dynamics simulations were carried out in an NVT ensemble at 298 K (Berendsen thermostat) for 100 ps (Materials Studio 6.1, Accelrys Company). Typically, the cutoff distance was 1.25 nm, and the isotropic periodic boundary condition was employed in the simulations.

**Characterization of RDX Crystals.** Morphology of RDX crystal was observed by optical microscopy (SMZ 745T, Nikon, Japan). The crystal structure of RDX crystal was investigated using an X-ray diffractometer (MiniFlex, Rigaku, Japan) operated at 30 kV and 15 mA with graphite-monochromatized Cu K$\alpha$ radiation ($\lambda$ = 1.5418 Å). Powder X-ray diffraction (PXRD) data were collected using a rotating flat-plate sample holder over the 2$\theta$ range from 10 to 50° with a step size of 0.02° and a scanning rate of 1.0°/min under ambient conditions.

## RESULTS AND DISCUSSION

**Induction Time Distribution of RDX with Oleylamine.** Figure 2 shows the induction times of RDX from acetone with a supersaturation ratio of 1.5 at 283.15 K. In general, nucleation is regarded as a stochastic process, and the present results of the induction time of RDX are also shown to be largely scattered: the range of induction times of RDX with no additive varies from 45 to 214 min (Figure 2a) and those with addition of oleylamine (Figure 2b), oleyl alcohol (Figure 2c), NDP (Figure 2d), and PVP (Figure 2e) are 23−90 min, 47−165 min, 30−147 min, and 96−384 min, respectively.

**Statistical Approach on Induction Time Distribution.** If the nucleation system were a simple homogeneous Poisson process, the probability of no nucleation, $N/N_0$, can be expressed as a function of the average induction time of homogeneous Poisson Process, $\tau_{homo}$, and time by the following equation:[20−24]

$$\frac{N(t)}{N_0} = \exp\left(-\frac{t}{\tau_{homo}}\right) \quad (1)$$


dx.doi.org/10.1021/cg4006423 | Cryst. Growth Des. 2013, 13, 4688−4694

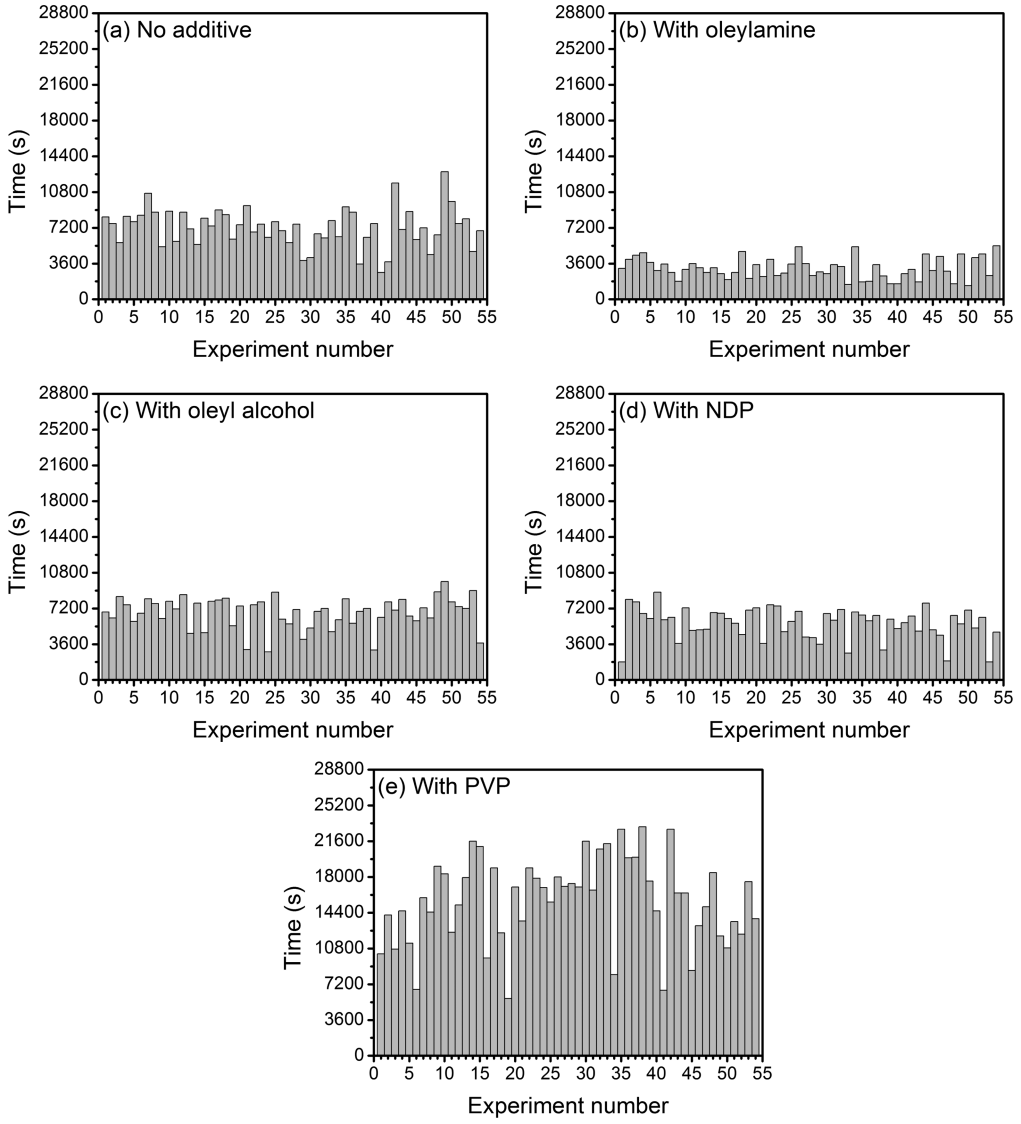


**Figure 2.** Induction time of 54 experiments for RDX (supersaturation ratio: $S$ = 1.5): (a) without additive, (b) with oleylamine, (c) with oleyl alcohol, (d) with NDP, and (e) with PVP.

Here the total number of isolated experiments, $N_0$, is 54, and $N$ is the number of experiments with no nucleation at time, $t$. In accordance with eq 1, the semilog plot of probability of no nucleation ($N/N_0$) as a function of time should be linear. However, as can be seen from Figure 3, the probability plots show a significant deviation from linearity with poor correlation coefficient (Table 1). If the growth rate were significantly slow, growth time of the nucleus to be detected induces an initial time lag of probability of no nucleation, $N/N_0$, but its linear dependency against time on the semilog plot is not changed in the classical nucleation process.[20]

On the other hand, the present experimental data (Figure 3) was found to be fitted with a compressed exponential model given by the following equation with an average induction time of nonhomogeneous Poisson process, $\tau$:[25−27]

$$\frac{N(t)}{N_0} = \exp\left(-\frac{t}{\tau}\right)^{\beta} \quad (2)$$

where $\beta$ is the compressed exponent. The deviation of the compressed exponent from unity reflects a nonhomogeneous Poisson process with a time-dependent rate. In the present system, the values of $\beta$ are shown to be quite greater than unity (Table 2), indicating that nucleation rate becomes faster as the experimental time elapses.[27]

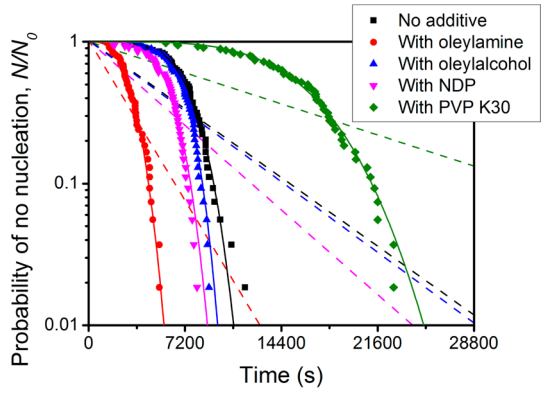


**Figure 3.** Semilog plot of probability of no nucleation with time at a constant supersaturation ratio, $S$, of 1.5 and additive concentration of 0.05 wt %. Dashed and solid curves were correlated by eqs 1 and 2, respectively.


dx.doi.org/10.1021/cg4006423 | Cryst. Growth Des. 2013, 13, 4688−4694

**Table 1. Average Induction Time of Homogeneous Poisson Process, $\tau_{homo}$, and Correlation Coefficients, $R^2$, of eq 1 at Supersaturation Ratio of 1.5**

| additive | $\tau_{homo}$ (s) | $R^2$ |
|---|---|---|
| no additive | 9510 | 0.53 |
| oleylamine | 4005 | 0.65 |
| oleyl alcohol | 8946 | 0.47 |
| NDP | 7419 | 0.56 |
| PVP | 20425 | 0.56 |

**Table 2. Average Induction Time of Nonhomogeneous Poisson Process, $\tau$, Compressed Exponent, $\beta$, and Correlation Coefficients, $R^2$, of eq 2**

| additive | $\tau$ (s) | $\beta$ | $R^2$ |
|---|---|---|---|
| no additive | 7822 | 4.683 | 0.99 |
| oleylamine | 3391 | 3.005 | 0.99 |
| oleyl alcohol | 7407 | 5.573 | 0.99 |
| NDP | 6328 | 4.519 | 0.99 |
| PVP | 17262 | 4.101 | 0.99 |

Mathematically, the growth time of the nucleus to be detected, $t_g$, may be incorporated into the nonhomogeneous Poisson Process equation:

$$\frac{N(t)}{N_0} = \exp\left(-\frac{t - t_g}{\tau}\right)^{\beta} \quad (3)$$

However, it is very difficult to estimate $t_g$ through mathematical fitting by eq 3 and the values of $\tau$ and $\beta$ obtained by fitting with eq 3 approach those values by eq 2 as $t_g$ becomes near zero. Therefore, the growth time of nucleus to be detected was not considered in the present analysis.

As shown in Figure 4 and Table 3, it is obvious that the nucleation rate increases and induction time decreases, respectively, with increasing supersaturation whether an additive is added or not.

**Nucleation Mechanism of RDX.** It is out of the scope of the present work to find a suitable nucleation mechanism of RDX, but we briefly note relationship between the probability distribution of induction time and theoretical nucleation kinetics. It has been well-known that the system limited by classical nucleation theory has the value of $\beta$ as unity and thus the present system cannot be described by that theory.[25−28] Recently, Toldy et al. reported that microdroplets formed by a microfluidic device were not perfectly isolated sometimes and they explained that $\beta$ was larger than unity as a result of nucleation trigger by the surrounding crystallized droplet.[27] However, the present crystallizing system isolated carefully by a glass reactor is not that case. When multiple crystallizers are employed, heterogeneous nucleation occurs first in crystallizers having impurities, and therefore, the probability of no nucleation, $N/N_0$, decreases as time elapses (i.e., $\beta$ should be smaller than unity).[28] This interpretation is opposite the present results, as shown in Tables 2 and 3.

The present results may be explained by the two-step nucleation theory, in which the effect of the structural organization of cluster into the ordered crystal lattice on the nucleation is considered as well as the growth of the cluster.[25,26] Kashchiev et al. proposed a two-step nucleation kinetics model, in which nucleation occurs only in the growing particle of an intermediate phase (growing cluster in this case), and revealed that nucleation can be delayed by the slow growth of the intermediate phases and/or by the slow nucleation of crystals in the intermediate phases.[29] This means that nucleation rate increases with time (i.e., $\beta$ is larger than unity). However, at this moment, it is difficult to show an experimental clue of the two-step nucleation in the present system, and we would prefer to reserve judgment.

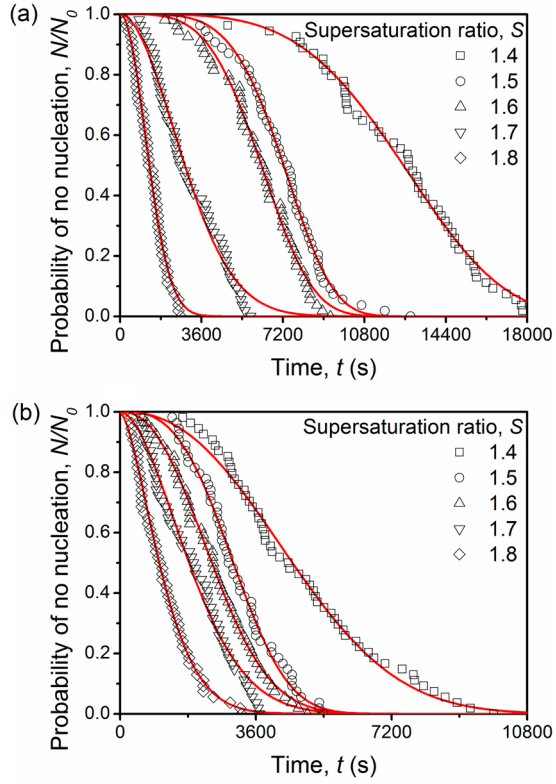


**Figure 4.** Probability of no nucleation of RDX in acetone at various supersaturation ratios with (a) no additive and (b) 0.05 wt % oleylamine. All curves are correlated by eq 2.

**Table 3. Average Induction Time of Nonhomogeneous Poisson Process, $\tau$, Compressed Exponent, $\beta$, and Correlation Coefficients, $R^2$, of eq 2 at Various Supersaturation Ratios**

| | no additive | | | with oleylamine | | |
|---|---|---|---|---|---|---|
| supersaturation ratio, S | $\tau$ (s) | $\beta$ | $R^2$ | $\tau$ (s) | $\beta$ | $R^2$ |
| 1.4 | 13710 | 4.049 | 0.99 | 5332 | 2.379 | 0.99 |
| 1.6 | 6855 | 3.942 | 0.99 | 2864 | 2.328 | 0.99 |
| 1.7 | 3460 | 1.924 | 0.98 | 2234 | 1.811 | 0.98 |
| 1.8 | 1549 | 2.025 | 0.99 | 1312 | 1.558 | 0.99 |

**Nucleation Promotion of RDX with Amphiphilic Additives.** Although nucleation rate of RDX is time-dependent, the average nucleation rate, $J$, could be calculated by $1/\tau V$. As shown in Table 2, the average induction time decreases with addition of oleylamine, oleyl alcohol, and NDP, thus those amphiphilic additives should be a nucleation promoter.

As can be seen from Figure 1c, the headgroup of oleyl alcohol may have a high affinity for the RDX molecule by the hydrogen bond of H(hydroxyl group)−O(RDX) and H-(hydroxyl group)−N(RDX). Although there is no hydrogen bond between RDX and NDP, the headgroup of NDP (lactam ring; see Figure 1d) is strongly polar because the carbonyl and tertiary amine groups, which are more electronegative than


dx.doi.org/10.1021/cg4006423 | Cryst. Growth Des. 2013, 13, 4688−4694

carbon, draw electron density away from the carbon.[30] In a similar manner, three nitro groups of RDX draw electron density away from 1,3,5-triazine, so RDX is also polar.[31] These polar molecules may have strong attractive electrostatic interactions between their opposite partial charges. *N*-methylpyrrolidone, whose molecular structure is similar to the headgroup of NDP, is a strong solvent for RDX, which also suggests that the headgroup of NDP has good affinity for RDX.[32]

As shown in Table 2, oleylamine should be a strong nucleation promoter more effective than oleyl alcohol. The structures of those two molecules with solute-philic functional headgroups and solute-phobic oleyl hydrocarbon chains are quite similar. Their solute-philic functional head groups, however, have different molecular affinities with RDX, which reflects solubility. Therefore, solubility measurements of RDX were made in solvents with similar functional groups, *n*-butylamine and *n*-butyl alcohol, and it was found that the solubility of RDX in *n*-butylamine ($3.764 \times 10^{-1}$ g/100 g *n*-butylamine) is much larger than that in *n*-butyl alcohol ($1.026 \times 10^{-2}$ g/100 g *n*-butyl alcohol) at 293.15 K. Those experimental results indicate that oleylamine has a stronger affinity to RDX than does oleyl alcohol. Therefore, the oleylamine molecule can easily anchor off the growing cluster of RDX. However, it is important to note that a strong amphiphilic additive does not always promote nucleation because excessively strong affinity between amphiphlic additive and growing cluster can retard nucleation because the interaction between solute and amphiphilic additives can induce a molecular complex, but, there is no general rule yet. The modeling work on the effect of affinity between amphiphilic additives and solute on nucleation induction time performed by Anwar et al.[6] showed an interesting result that both too strong and too weak affinity between solute and amphiphilic additives slows down nucleation.

It is interesting to note that NDP acts as a nucleation promoter of RDX, whereas PVP as a nucleation retarder, even NDP and PVP, have the same solute-philic functional headgroup, as shown in Figure 1 (panels d and e). As mentioned above, solute-philic polymer additives can interact with solutes at any direction and hinder the packing of solute molecules into a crystal lattice like the RDX/PVP system. However, solute-philic headgroup of NDP strongly interacts with the RDX cluster, and the hydrocarbon tail of NDP can cover surface of the RDX cluster without disruption of packing into the crystal structure. This environment may induce a remarkable difference in nucleation induction times of RDX.

**Molecular Simulation of RDX Aggregation Pattern.** Figure 5 shows the molecular simulation results on the aggregation pattern of RDX molecules with some additive molecules. It should be noted that the present simulation work is only to show the aggregation pattern of RDX with additives, not the actual nucleation event. Therefore, the additive concentration was set larger than that in the actual experimental condition. It was found that the solute-philic headgroup of amphiphilic molecules is strongly attached on the surface of the RDX aggregate like an anchor, whereas the hydrocarbon chain covered the surface of the aggregate, as can be seen from Figure 5 (panels a–c). These patterns are geometrically similar to the modeling result with an amphiphilic dimer by Anwar et al.[5−7] However, interaction of PVP molecules with the RDX cluster seem to be quite different from those configurations. As shown in Figure 5d, the PVP molecule cannot cover the RDX aggregate but penetrate into the RDX aggregates because PVP can interact strongly with RDX in every direction.

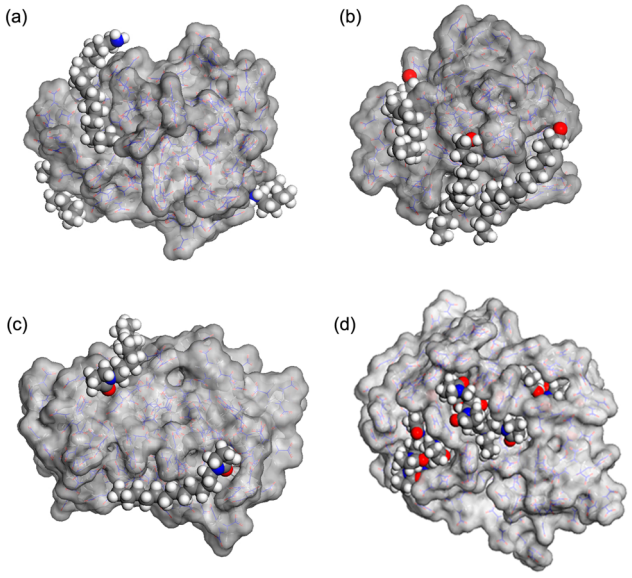


**Figure 5.** Aggregation patterns of RDX molecules with (a) oleylamine, (b) oleyl alcohol, (c) NDP, and (d) PVP (repeat unit: $n = 15$) molecules. Initially, 150 RDX molecules and 6 nucleation agents were randomly distributed in a vacuum cubic cell of $8.3 \times 8.3 \times 8.3$ nm$^3$. Nucleation agent molecules are represented by ball notation, and RDX molecules are represented by stick notation in the Connolly surface for the ease of understanding. Colors of atoms in packing: carbon (dark gray), nitrogen (blue), oxygen (red), and hydrogen (white).

**Effect of Amphiphilic Additives on Morphology and Polymorphism of RDX Crystals.** Morphology of RDX crystal obtained from acetone has been reported to be as prismlike, and the major faces are four trapezoid broad faces of {210} planes and eight isosceles triangle faces of {111} planes.[33,34] We also obtained the prismlike RDX crystal from acetone, as shown in Figure 6a, and it was found that there is no significant morphological change by addition of amphiphilic additives, as can be seen from Figure 6 (panels b–d).

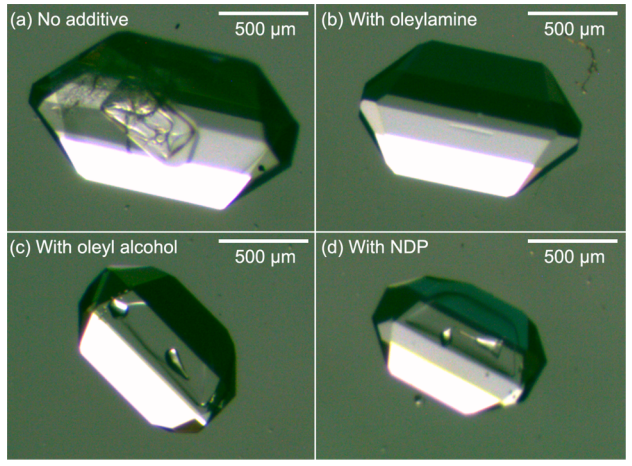


**Figure 6.** Optical microphotographs of RDX crystals obtained from experiments for induction time measurement at supersaturation ratio, *S*, of 1.5 with (a) no additive, (b) oleylamine, (c) oleyl alcohol, and (d) NDP.


dx.doi.org/10.1021/cg4006423 | *Cryst. Growth Des.* 2013, 13, 4688−4694

In the solid state, RDX is known to have at least 5 polymorphs ($\alpha$, $\beta$, $\gamma$, $\delta$, and $\varepsilon$) and the $\alpha$-form is thermodynamically stable in ambient condition among those polymorphs.[35−39] All RDX crystals obtained in the present work are $\alpha$-form (Figure 7), showing that all additives have no influence on the crystal structure of RDX.

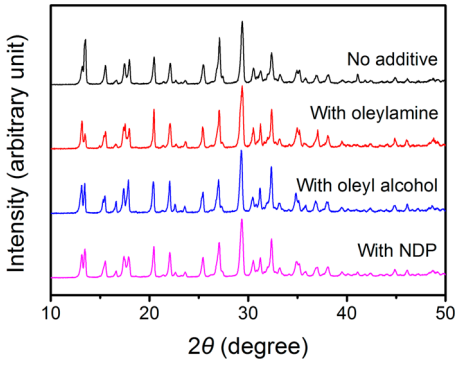


**Figure 7.** Powder X-ray diffraction (PXRD) patterns of RDX crystals obtained from experiments for induction time measurement at supersaturation ratio, *S*, of 1.5.

## CONCLUSIONS

Amphiphilic molecules such as oleylamine, oleyl alcohol, and NDP were experimentally evidenced to act as a nucleation promoter in the crystallization of RDX from acetone by measurements of induction time. Molecular simulation on the aggregation patterns of RDX with those nucleation agents supports that the solute-philic headgroup of amphiphilic molecules is easily embedded onto the surface of a clusterlike anchor, but the solute-phobic hydrocarbon chain covers the surface of the cluster. Those results would be useful for the design of nucleation agents for the promotion of nucleation for many purposes (e.g., purity and inclusion control), selective separation of a specific crystal phase, morphology control of spray-assisted evaporation crystallization, etc.[1,18,40,41] One limit of the present work is that reduction of the interfacial energy by nucleation promoters could not be verified experimentally because most induction time models to estimate the interfacial energy are originated from classical nucleation theory, which is expressed by the homogeneous Poisson process.

## AUTHOR INFORMATION

### Corresponding Author

*E-mail koo@sogang.ac.kr. Tel: +82-2-705-8680. Fax: +82-2-711-0439.

### Notes

The authors declare no competing financial interest.

## ACKNOWLEDGMENTS

This work was supported by Hanwha and Agency for Defense Development (UC120019GD; Republic of Korea) and by the Human Resources Development program (Grant 20114010203090) of the Korea Institute of Energy Technology Evaluation and Planning (KETEP) grant funded by the Korea government Ministry of Trade, Industry and Energy.

## REFERENCES

(1) Vekilov, P. G. *Cryst. Growth Des.* **2010**, *10*, 5007.
(2) Sangwal, K. *Additives and Crystallization Processes From Fundamentals to Applications*; John Wiley & Sons, Ltd: Chichester, West Sussex, England, 2007.
(3) Sangwal, K. *J. Cryst. Growth* **2009**, *311*, 4050.
(4) Sangwal, K. *J. Cryst. Growth* **2010**, *312*, 3316.
(5) Anwar, J.; Zahn, D. *Angew. Chem., Int. Ed.* **2011**, *50*, 1996.
(6) Anwar, J.; Boateng, P. K.; Tamaki, R.; Odedra, S. *Angew. Chem., Int. Ed.* **2009**, *48*, 1596.
(7) Song, R.-Q.; Cölfen, H. *CrystEngComm* **2011**, *13*, 1249.
(8) Stepanov, V.; Krasnoperov, L. N.; Elkina, I. B. *Propellants, Explos., Pyrotech.* **2005**, *30*, 178.
(9) Lee, B.-M.; Jeong, J.-S.; Lee, Y.-H.; Lee, B. C.; Kim, H.-S.; Kim, H.; Lee, Y.-W. *Ind. Eng. Chem. Res.* **2009**, *48*, 11162.
(10) Yang, G.; Nie, F.; Huang, H.; Zhao, L.; Pang, W. *Propellants, Explos., Pyrotech.* **2005**, *31*, 390.
(11) Teipel, U. *Propellants, Explos., Pyrotech.* **1999**, *24*, 134.
(12) Teipel, U.; Kröber, H.; Krause, H. H. *Propellants, Explos., Pyrotech.* **2001**, *26*, 168.
(13) Spitzer, D.; Baras, C.; Schäfer, M. R.; Ciszek, F.; Siegert, B. *Propellants, Explos., Pyrotech.* **2011**, *36*, 65.
(14) Radacsi, N.; Stankiewicz, A. I.; Creyghton, Y. L. M.; van der Heijden, A. E. D. M.; ter Horst, J. H. *Chem. Eng. Technol.* **2011**, *34*, 624.
(15) Huang, H.; Wang, J.; Xu, W.; Xie, R. *Propellants, Explos., Pyrotech.* **2009**, *34*, 78.
(16) Qiu, H.; Stepanov, V.; Di Stasio, A. R.; Chou, T.; Lee, W. Y. *J. Hazard. Mater.* **2011**, *185*, 489.
(17) Essel, J. T.; Cortopassi, A. C.; Kuo, K. K.; Leh, C. G.; Adair, J. H. *Propellants, Explos., Pyrotech.* **2012**, *37*, 699.
(18) Kim, J.-W.; Shin, M.-S.; Kim, J.-K.; Kim, H.-S.; Koo, K.-K. *Ind. Eng. Chem. Res.* **2011**, *50*, 12186.
(19) Kim, K.-J.; Mersmann, A. *Chem. Eng. Sci.* **2001**, *56*, 2315.
(20) Jiang, S.; Horst, ter, J. H. *Cryst. Growth Des.* **2011**, *11*, 256.
(21) Diao, Y.; Myerson, A. S.; Hatton, T. A.; Trout, B. L. *Langmuir* **2011**, *27*, 5324.
(22) Diao, Y.; Helgeson, M. E.; Myerson, A. S.; Hatton, T. A.; Doyle, P. S.; Trout, B. L. *J. Am. Chem. Soc.* **2011**, *133*, 3756.
(23) Diao, Y.; Whaley, K. E.; Helgeson, M. E.; Woldeyes, M. A.; Doyle, P. S.; Myerson, A. S.; Hatton, T. A.; Trout, B. L. *J. Am. Chem. Soc.* **2012**, *134*, 673.
(24) Diao, Y.; Helgeson, M. E.; Siam, Z. A.; Doyle, P. S.; Myerson, A. S.; Hatton, T. A.; Trout, B. L. *Cryst. Growth Des.* **2012**, *12*, 508.
(25) Knezic, D.; Zaccaro, J.; Myerson, A. S. *J. Phys. Chem. B* **2004**, *108*, 10672.
(26) Erdemir, D.; Lee, A. Y.; Myerson, A. S. *Acc. Chem. Res.* **2009**, *42*, 621.
(27) Toldy, A. I.; Badruddoza, A. Z. M.; Zheng, L.; Hatton, T. A.; Gunawan, R.; Rajagopalan, R.; Khan, S. A. *Cryst. Growth Des.* **2012**, *12*, 3977.
(28) Teychené, S.; Biscans, B. *Cryst. Growth Des.* **2011**, *11*, 4810.
(29) Kashchiev, D.; Vekilov, P. G.; Kolomeisky, A. B. *J. Chem. Phys.* **2005**, *122*, 244706.
(30) Aparicio, S.; Alcalde, R.; Dávila, M. J.; García, B.; Leal, J. M. *J. Phys. Chem. B* **2008**, *112*, 11361.
(31) Zhurov, V. V.; Zhurova, E. A.; Stash, A. I.; Pinkerton, A. A. *Acta Crystallogr., Sect. A* **2011**, *67*, 160.
(32) Sitzmann, M. E.; Foti, S. C. *J. Chem. Eng. Data* **1975**, *20*, 53.
(33) ter Horst, J. H.; Geertman, R. M.; van der Heijden, A. E.; van Rosmalen, G. M. *J. Cryst. Growth* **1999**, *198*, 773.
(34) Zhang, C.; Ji, C.; Li, H.; Zhou, Y.; Xu, J.; Xu, R.; Li, J.; Luo, Y. *Cryst. Growth Des.* **2013**, *13*, 282.
(35) Choi, C. S.; Prince, E. The Crystal Structure of Cyclotrimethy - lenetrinitramine. *Acta Crystallogr.* **1972**, *B28*, 2857−2862.
(36) Karpowicz, R. J.; Sergio, S. T.; Brill, T. B. *Ind. Eng. Chem. Prod. Res. Dev.* **1983**, *22*, 363−365.
(37) Dreger, Z. A.; Gupta, Y. M. *J. Phys. Chem. B* **2007**, *111*, 3893−3903.
(38) Dreger, Z. A.; Gupta, Y. M. *J. Phys. Chem. A* **2010**, *114*, 7038−7047.

(39) Dreger, Z. A.; Gupta, Y. M. *J. Phys. Chem. A* **2010**, *114*, 8099–8105.
(40) Cao, X.; Duan, X.; Pei, C. *Cryst. Res. Technol.* **2013**, *48*, 29.
(41) Kim, J.-W.; Kim, J.-K.; Kim, H.-S.; Koo, K.-K. *Cryst. Growth Des.* **2009**, *9*, 2700.